Multiphoton multiple ionisation of N_2O probed by three-dimensional covariance mapping

L.J. Frasinski, P.A. Hatherly and K. Codling
J.J. Thomson Physical Laboratory, Whiteknights, P.O. Box 220, Reading RG6 2AF, Berks., UK

Received 26 February 1991; accepted for publication 15 April 1991
Communicated by B. Fricke

One can attempt to understand the complex dynamics of multiphoton multiple ionisation of triatomic molecules using conventional time-of-flight mass spectrometry, but only by applying three-dimensional covariance mapping can processes involving the simultaneous production of three charged fragments be unequivocally assigned to a specific parent molecular ion.

When homonuclear diatomic molecules such as N_2 are multiply ionised using an intense subpicosecond laser, any attempt at analysis of the resulting fragmentation pattern using time-of-flight (TOF) mass spectrometry is seriously compromised by an inability to differentiate the asymmetric processes involving neutral fragments, for example $[N_2^{2+}] \rightarrow N + N^{2+}$, from the symmetric ones, namely $[N_2^{4+}] \rightarrow N^{2+} + N^{2+}$. Equally, it is difficult to analyse TOF spectra of heteronuclear molecules such as CO if identical fragment atomic ions from different parent molecular ions have similar energies. These problems have been alleviated recently by the introduction of two-dimensional covariance mapping, which allows unequivocal correlation of fragment ion pairs with parent molecular ions [1,2] and thereby a more complete description of the dynamics of laser–molecule interactions.

In the case of the multiphoton multiple ionisation of triatomic molecules the situation is much more complex. One can produce similar two-dimensional covariance maps but these only serve to indicate correlations between pairs of fragment ions, whereas at the higher laser intensities it is quite probable that three correlated fragment ions will be produced. Although one might infer from a combination of one-dimensional TOF spectra and two-dimensional covariance maps that three ions have been created simultaneously, the only sure way of confirming a triple-ion process is by using three-dimensional covariance mapping. This Letter intends to show that such confirmation has been possible in the case of N_2O.

In the experiments described here, a laser of wavelength 600 nm, pulse length 0.6 ps, repetition rate 10 Hz and focused intensity somewhat in excess of 10^{15} W/cm^2, is used to multiply ionise an assembly of N_2O molecules. A field across the interaction region accelerates the ions towards a short drift tube and thence to a pair of microchannel plate detectors [3]. The ion signal is fed directly to a digital oscilloscope and fig. 1 is typical of the TOF spectra obtained. In this case the E field of the linearly polarised laser beam lies along the axis of the drift tube. In the field ionisation model [4] a diatomic molecule is more easily ionised when its molecular axis lies along the laser E field. A similar behaviour is expected for linear triatomic molecules such as N_2O. Since there is little time for molecular rotation, the ions will also be ejected preferentially along the drift tube axis, either towards ("forward" ions) or away from ("backward" ions) the microchannel plates.

The forward ions have TOFs that vary linearly with momentum component along the drift tube axis. The kinetic energy scales beneath the spectrum refer to these ions and were obtained by computer simulation of the well-characterised drift tube. The backward ions, of identical energy range, reverse their

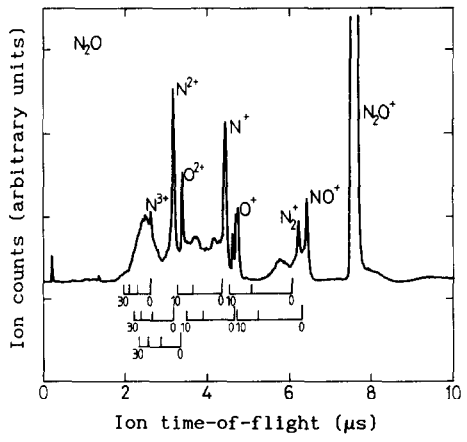

Fig. 1. TOF spectrum of N_2O. The sharp peaks are associated with "backward" fragment ions. The connection between a particular group of "forward" ions and its energy scale is made by noting that each backward peak lies just to the right of the 0 eV position.

trajectories in the applied field and arrive almost simultaneously at the microchannel plates, regardless of their initial kinetic energies. These produce the sharp peaks in the TOF spectrum and their appearance allows immediate identification of the various fragment ions present in the focal region of the laser.

By observing the movement of the forward ion peaks as a function of the voltage, one can attempt to analyse the spectrum. However, with broad or weak features, it has proved impossible to make unambiguous determination of the kinetic energy and charge state of the various ions. For example, the broad feature at about 2.5 μs is due to overlapping N^{2+} and O^{2+} ions but it was difficult to quantitatively apportion the peak to these two species. Each ion has an energy peak at about 20 eV. At this point the covariance mapping technique was applied in order to allow correlation of pairs of charged particles. To achieve this, a new drift tube was constructed [5], a factor of two shorter than that used to produce fig. 1. This ensured 100% collection efficiency of forward *and* backward ions but at the expense of energy resolution. It also had the important feature that the ion TOF was a linear function of momentum component along the drift tube axis for both forward and backward ions.

The principle of covariance mapping has been described elsewhere [1] but a brief reminder is presented here. Suppose that for a given laser pulse, the following two-body fragmentation process occurs:

$$N_2O + nh\nu \rightarrow [N_2O^{2+}] \rightarrow N_b^+ + NO_f^+ ,$$

where subscripts f and b refer to forward and backward ions. If the N_b^+ fragment is detected at TOF t_1, there is an enhanced probability of detecting an NO_f^+ fragment at TOF t_2. This probability is considerably less than 100% because of poor detector efficiency. When one calculates, over many laser pulses, the covariance between the TOF points at which the fragments are detected, one obtains a positive value. This is given by the expression

$$C(t_1, t_2) = \langle X(t_1)\, X(t_2)\rangle - \langle X(t_1)\rangle \langle X(t_2)\rangle ,$$

where X is the amplitude of the digitised signal. (In general $C = \langle XY\rangle - \langle X\rangle\langle Y\rangle$, where X and Y denote two different signals, but here $X = Y$ because only one detector is involved.) Because one does not know in advance which points on the TOF spectrum are correlated, one calculates the covariance for each pair (t_1, t_2) of TOF points (channels in the digital oscilloscope) and presents it in the form of a two-dimensional map such as fig. 2a.

The linear relationship between TOF and momentum component along the drift tube axis suggests that the covariance map should be seen as a momentum correlation diagram. In the above two-body fragmentation, momentum conservation dictates that the correlated structure be in the form of a line. The two islands in the top right-hand corner of fig. 2a reflect the forward–backward and backward–forward fragments correlations. In order to allow the reader to recognise these correlations, a time-averaged, one-dimensional TOF spectrum is shown on the ordinate and abscissa. One sees that the upper of the two features involves N_f^+ and NO_b^+ ions, whereas the lower involves N_b^+ and NO_f^+ ions (the order denotes ions on the x and y axes respectively). The tilt of the blue line, in this case 45°, gives the ion charge ratio and the intensity variation along the line gives the momentum distribution and hence the energy spread. Although the features are rather weak, one finds that the NO^+ ions have an energy range of 1.5 to 2.0 eV and, through momentum conservation, the N^+ ions must have an energy range of 3.2 to 4.3 eV. The computer simulation in fig. 2b, alongside, gives the relevant correlations, the "length" of each

island relating roughly to the momentum spread.

The above channel is clearly a minor one when compared to that responsible for the six main features in fig. 2a. The strong red line at 45° is the autocorrelation line and is of no real interest here except that one obtains reflection symmetry in this line. Because of their location on the map (i.e. on the TOF spectrum), the features must be associated with doubly-charged ions. However, as pointed out in the introduction, any analysis using two-dimensional covariance mapping is bound to be ambiguous because one cannot differentiate the situation where pairs of ions are produced independently:

$$N_2O + nh\nu \rightarrow [N_2O^{4+}] \rightarrow N^{2+} + N_m^{2+} + O$$

or

$$\rightarrow N + N_m^{2+} + O^{2+}$$

or

$$\rightarrow N^{2+} + N_m + O^{2+} ,$$

from the situation where three ions are produced simultaneously:

$$N_2O + nh\nu \rightarrow [N_2O^{6+}] \rightarrow N^{2+} + N_m^{2+} + O^{2+} .$$

The subscript m denotes the middle N atom of N_2O ($N \equiv N_m = O$).

In order to remove this ambiguity, a three-dimensional covariance map is required. In this case one is looking for correlations between three points (t_1, t_2, t_3) in the TOF spectrum. The following expression is a natural extension to the two-dimensional case discussed earlier:

$$\begin{aligned} C(t_1, t_2, t_3) = {} & \langle X(t_1)\, X(t_2)\, X(t_3) \rangle \\ & - \langle X(t_1)\, X(t_2) \rangle \langle X(t_3) \rangle \\ & - \langle X(t_1)\, X(t_3) \rangle \langle X(t_2) \rangle \\ & - \langle X(t_2)\, X(t_3) \rangle \langle X(t_1) \rangle \\ & + 2 \langle X(t_1) \rangle \langle X(t_2) \rangle \langle X(t_3) \rangle . \end{aligned}$$

This expression must be evaluated at all possible times t_1, t_2 and t_3 in the TOF spectrum in order to produce the three-dimensional map depicted schematically in fig. 2d. There is one autocorrelation line, where $t_1 = t_2 = t_3$, and three autocorrelation planes, where $t_1 = t_2$, $t_2 = t_3$ and $t_1 = t_3$; these are shown hatched in the figure. Moreover, the map has three mirror symmetries with respect to these autocorrelation planes, giving sextuple repetition of any feature (circles in fig. 2d).

Apart from the autocorrelation planes themselves and any statistical noise, *only true triple fragment correlations* will give real counts on the map. The six 3D correlation features corresponding to a single triple fragmentation channel, lie in a plane (the hexagon shown in fig. 2d) defined by momentum conservation. Since the momentum component along the drift tube axis is linearly related to the TOF (t), these 3D features will occur at the following (x, y, z) coordinates: (t_1, t_2, t_3), (t_1, t_3, t_2), (t_2, t_1, t_3), (t_2, t_3, t_1), (t_3, t_1, t_2) and (t_3, t_2, t_1). If one looks down on the cube from above, one sees the six features in the two-dimensional map, fig. 2a.

In order to locate a specific 3D feature one takes slices of the three-dimensional covariance map. One is guided to the approximate location of one of these features by the two-dimensional map. One such slice is shown schematically in fig. 2d. (The red lines indicate where the autocorrelation planes cut through the slice.) If real, the feature should appear and disappear as one takes slices at increasing values of z. Examination of a number of such slices (18 are shown in fig. 2c) confirms that the feature is most obvious at $z = 0.89$ μs. Note that the feature lies at coordinates $x \approx 1.09$ μs and $y \approx 0.73$ μs, consistent with fig. 2a. Inevitably there is a price to pay for adding a third dimension to the map. The signal-to-noise deteriorates, reflecting the fact that the covariance signal involves a triple product of detector efficiency (20–30%), rather than a double product.

Having confirmed that the main structures in fig. 2a are indeed due to a single triple-fragmentation process, a "best fit" is made to the data, see fig. 2b. One notes that, rather than the six features discussed so far, there are twelve in all. This occurs because of the "forward–backward" and "backward–forward" momentum symmetry discussed earlier. In this instance the features group into six rather poorly resolved pairs because of the low momentum of the middle (N_m^{2+}) ion. For example, the sharp feature at about 45° situated below the autocorrelation line consists of two features: (N_b^{2+}, O_f^{2+}) and (O_b^{2+}, N_f^{2+}), where the order denotes fragment ions on the (x, y) axes. The table beneath the figure gives the most consistent picture of the fragmentation, show-

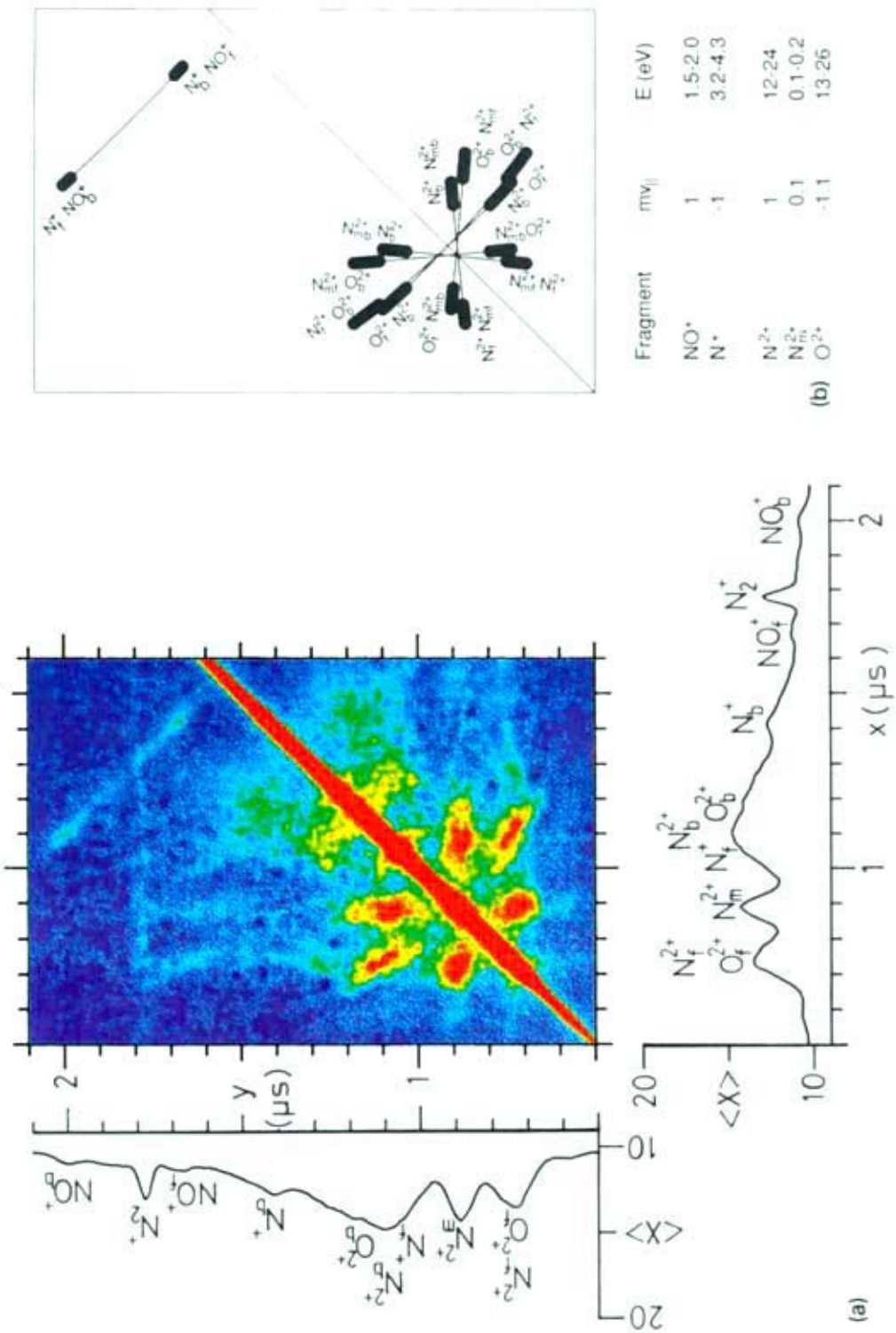

Fig. 2. (a) Two-dimensional map of N_2O. The conventional time-averaged TOF spectrum is placed along the x and y axes. (b) Simulation of the two-dimensional map, see text for labelling. The table beneath gives the energy range of the ions. (c) Slices of the three-dimensional map. One such slice is shown schematically in (d). The rectangle at the bottom right indicates the range of x and y; the values of z are given above each slice. (d) A schematic three-dimensional map. The origin is at $x=y=z=0.6$ μs and the cube extends to 1.2 μs. The strong red lines on the slice show intersections with the hatched autocorrelation planes.

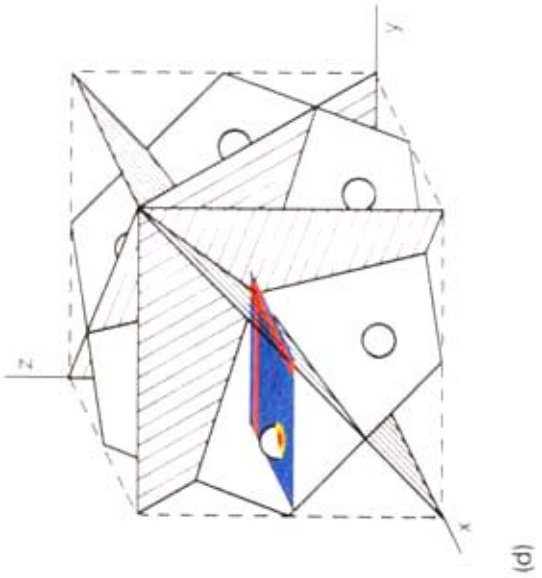

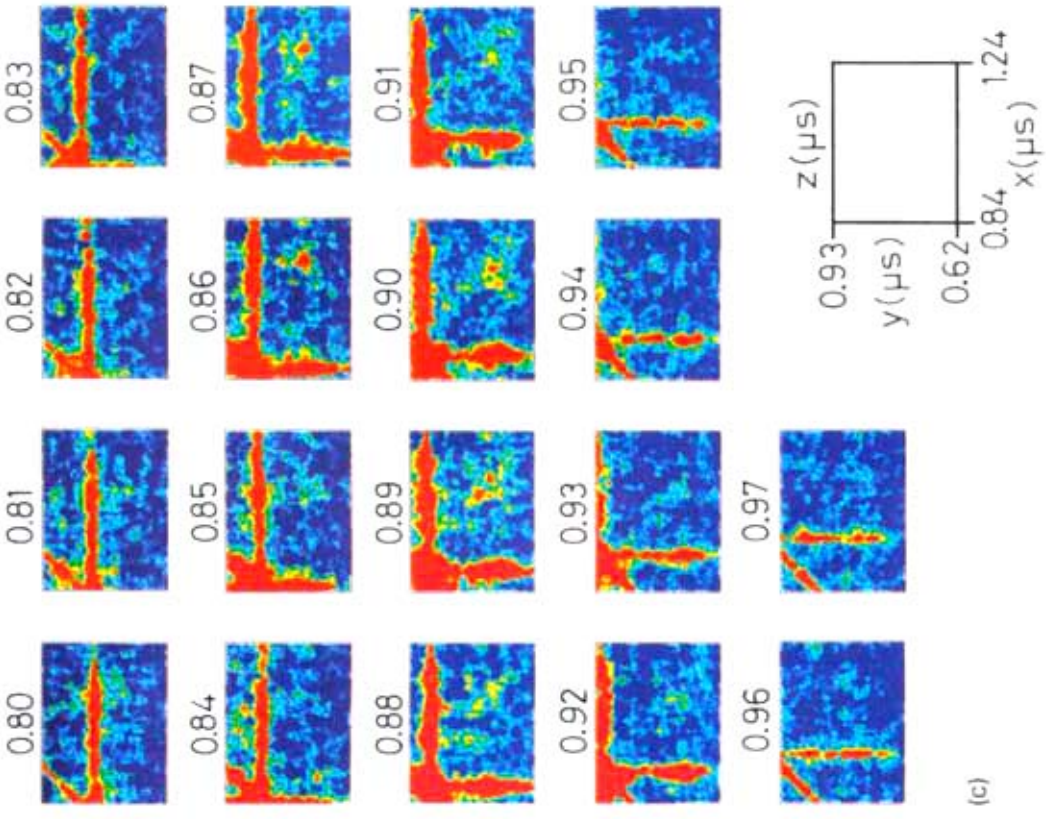

Fig. 2. (continued).

ing the momentum of each ion along the drift tube axis and the associated energy range.

Clearly, momentum must be conserved along the axis, and one finds the momentum of the N_m^{2+} ion to be one tenth of that of the N^{2+} ion, with the N_m^{2+} ion moving slowly in the same direction as the N^{2+} ion. This is what might have been expected and is what is also seen in single-photon ionisation at 470 eV [6]. The mean energies of the ions are as follows: $N^{2+} \approx 18$ eV; $N_m^{2+} \approx 0.15$ eV; $O^{2+} \approx 20$ eV. By rotating the E vector of the laser through 90°, one can measure the momentum component of the various fragment ions in a direction perpendicular to the E vector [6]. The resulting covariance maps indicate that these components are small, consistent with the field ionisation model.

The fit of the "Coulomb explosion" momenta, fig. 2b, to the experimental map, fig. 2a, is not perfect. One might be tempted to improve the fit by assuming three independent two-fragment-ion processes. In each of these processes the third neutral particle could be allowed to take away any momentum along the drift tube axis that one cares to assign to it. However, the 3D map reveals that triple-ion fragmentation is the major channel. Any remaining disagreement between figs. 2a and 2b must therefore be attributed to poor statistics. There are few signs of $N^+ + N^+$, $N^+ + O^+$ or $N^+ + N^{2+}$ channels above the noise. The feature lying close to the autocorrelation line at about 1.2 μs is associated with $C^+ + C^+$ correlations from hydrocarbon impurities.

The total kinetic energy release (about 38 eV) seems to suggest that, as the three atoms move apart and as the laser field increases towards its peak value, there comes a point when the "molecule" is suddenly six times ionised. If one assumes a simple model of mutual Coulomb repulsion, the atoms must be at least three times their normal internuclear separation at the time of multiple ionisation. It is puzzling that correlations involving single ions are so weak. For example, one might have expected to observe substantial features associated with the process $[N_2O^{3+}] \rightarrow N^+ + N_m^+ + O^+$; this would occur in regions around the focal spot. One is led to speculate that, as the laser E field increases, six electrons are successively or collectively promoted to dynamic states of a new kind, stabilised by a combination of the oscillating E field and the three potential wells. As the laser field increases to a point where stability can no longer be sustained, all six electrons are ejected simultaneously and three double-ions are produced. Clearly this interesting phenomenon deserves further investigation.

In conclusion, we have indicated how three-dimensional covariance mapping allows analysis of complex one-dimensional TOF spectra, involving three correlated charged fragments. Although the technique has been applied here to the multiphoton regime, there is no reason, in principle, why it cannot be used in single photon multiple ionisation. Indeed, covariance mapping should be seen as a general technique, applicable in many diverse situations where correlations are suspected.

We are pleased to acknowledge the Science and Engineering Research Council (UK) for their financial support and the use of the Laser Support Facility. We are indebted to Drs. W.T. Toner and I.N. Ross of Rutherford Appleton Laboratory for providing the focused laser.

References

[1] L.J. Frasinski, K. Codling and P.A. Hatherly, Science 240 (1989) 1029.
[2] L.J. Frasinski, K. Codling and P.A. Hatherly, Phys. Lett. A 142 (1989) 499.
[3] K. Codling, L.J. Frasinski and P.A. Hatherly, J. Phys. B 20 (1987) L525.
[4] K. Codling, L.J. Frasinski and P.A. Hatherly, J. Phys. B 22 (1989) L321.
[5] P.A. Hatherly, L.J. Frasinski, K. Codling, A.J. Langley and W. Shaikh, J. Phys. B 23 (1990) L291.
[6] D.M. Hanson, C.I. Ma, K. Lee, D. Lapiano-Smith and D.Y. Kim, J. Chem. Phys. 93 (1990) 9200.